A High-Power Lithium-Sulfur Battery combining Catholyte and Composite Cathode

Edoardo Barcaro [a] and Jusef Hassoun [a, b*]

[a] University of Ferrara, Department of Chemical, Pharmaceutical and Agricultural Sciences, Via Fossato di Mortara 17, 44121, Ferrara, Italy.

[b] Graphene Labs, Istituto Italiano di Tecnologia, via Morego 30, Genova, 16163, Italy

*Corresponding author: jusef.hassoun@unife.it , jusef.hassoun@iit.it

Keywords:

Li-deficient polysulfide • S-Sn-MnO_2 electrode • High-power • High-current • Li-S battery

Supplementary Information

Contains 7 Figures and 2 Tables

Experimental Section

Preparation of the catholyte

The liquid catholyte was prepared by dissolving into a sealable bottle elemental sulfur (2.244 g, 0.07 mol, ≥ 99.5 %, Riedel-de-Haën) and Li_2S (0.322 g, 0.07 mol, 99.98 %, Sigma-Aldrich) in 11 ml (9.548 g) of dioxolane (DOL anhydrous, contains ca. 75 ppm BHT as inhibitor, 99.8 %, Sigma-Aldrich) and 11 ml (9.660 g) of dimethoxyethane (DME anhydrous, 99.5 %, inhibitor-free, Sigma-Aldrich). After sealing the bottle an orange suspension was achieved, which was stirred for 6 h at 70 °C and for two days at room temperature to obtain a precursor looking intense red at the end of the process (see Figure S1). The temperature was checked with the aid of a thermocouple, and maximum fluctuation of ± 2.0 °C was experienced. The used amounts of Li_2S and S were selected to get the Li-deficient catholyte with a stoichiometry of $Li_{1.5}S_8$ instead the common one (Li_2S_8). The sulfur content in 10 µL of catholyte was 0.878 mg, corresponding to a ratio with respect of the catholyte weight of 7.14 %. Before using, the solvents were dried under molecular sieves (rods, 3 Å, size 1/16 inch, Honeywell Fluka) until the water content was below 10 ppm, as tested through 899 Karl Fischer Coulometer (Metrohm). Lithium bis(trifluoromethanesulfonyl)imide (LiTFSI, $LiN(SO_2)_2(CF_3)_2$, 99.95 % trace metals basis, Sigma-Aldrich) and $LiNO_3$ (99.99 % trace metals basis, Sigma-Aldrich) were dissolved in the precursor by stirring for 12 h at room temperature, to get a concentration of 1 mol of each salt in 1 kg of DOL:DME solvent mixture. Before employment, LiTFSI and $LiNO_3$ were dried for 2 days under vacuum at 110 °C. A control electrolyte consisted of a solution formed by DOL and DME solvents mixed in the 1:1 weight ratio, LiTFSI and $LiNO_3$ in a 1 mol $kg_{solvent}^{-1}$ concentration for each salt. The catholyte and control electrolyte have been prepared inside an Ar-filled glovebox (MBraun, O_2 and H_2O content below 1 ppm).

Figure S1. Photograpic images taken upon the catholyte preparation. Left panel shows the first stage of the process, right panel displays the precursor after 7 h stirring at 70 °C and 48 h stirring at room temperature just before salts addition.

Electrochemical characterization of the catholyte

The electrochemical features of catholyte solution were studied in CR2032 coin-type cells (MTI Corp.) assembled in an Ar-filled glovebox. The ionic conductivity was investigated by means of electrochemical impedance spectroscopy (EIS) in the 500 kHz – 100 Hz frequency range through an alternate voltage signal of 10 mV on blocking-electrode stainless-steel|catholyte solution|stainless-steel symmetrical cells containing one O-rings (23-5FEP-2-50, CS Hyde, internal diameter of 10 mm, thickness of 127 µm) holding the catholyte to fix the cell constant at 0.016 cm^{-1}. The temperature of the cell ranged from 0 up to 64.1 °C and was controlled via a F 12 Julabo instrument (double-checked with a thermocouple). The Li^+ transference number (t^+) was evaluated by applying the Bruce-Vincent-Evans method (see ref 10 in Manuscript). A symmetrical cell with Li|catholyte|Li configuration was prepared by stacking two 14 mm-diameter lithium discs (0.25 mm thickness, MTI Corp.) separated by an 18 mm-diameter Celgard 2500 monolayer microporous membrane disc soaked with 50 µL of catholyte solution. A chronoamperometry test was carried out on the cell by applying a voltage (ΔV) of 0.03 V for 90 min, and EIS was performed before and after polarization using the 500 kHz – 100

mHz frequency range and an alternate voltage signal of 10 mV. The voltage, currents, and resistance values were used in equation (2) in Manuscript to calculate t^+. An identical cell configuration as above was used to investigate the lithium/catholyte interphase stability upon aging at room temperature, by performing EIS measurements every 2 h for the first 14 h since assembly, and daily during the following 14 days, using the 500 kHz – 100 mHz frequency range and 10 mV alternate voltage signal. Carbon electrodes were prepared through doctor blade casting on a gas diffusion layer foil (GDL ELAT 1400, 454 μm thickness) of a slurry obtained by dispersing carbon black (90 %, Super P carbon, Timcal) and polyvinylidene fluoride (10 %, PVDF, Solef 6020) polymer binder in *N*-methyl-2-pyrrolidone (NMP, Sigma-Aldrich). The wet foil was dried on a hot plate at 70°C, cut into 14 mm diameter discs, dried for 3 h at 110°C under vacuum inside a Büchi oven, and subsequently stored inside an Ar-filled glovebox. The electrochemical stability window of catholyte solution was determined by linear sweep voltammetry (LSV) measurements on Li|50 μL catholyte solution|Carbon coin-cells (CR2032, MTI corp.) from the open circuit voltage (OCV) to 5.0 or 0.01 V *vs.* Li^+/Li at 0.1 mV s^{-1}. The cells used a 14 mm-diameter lithium disc (0.25 mm thick, MTI corp.) separated by one 18 mm-diameter membrane (Celgard 2500) from a 14 mm-diameter carbon electrode soaked with 66 μL of catholyte (containing 5.8 mg of S). The electrochemical process was studied through cyclic voltammetry (CV), which was performed within 2.1 − 2.8 V *vs.* Li^+/Li at a scan rate of 0.1 mV s^{-1}. Prior to this measurement, the cell was galvanostatically charged from the OCV to 2.8 V, using a current of C/10 (1C = 419 mA g_S^{-1}). LSV, CV and EIS tests were carried out by a VersaSTAT MC Princeton Applied Research (PAR-AMETEK) instrument at room temperature (25 °C), while galvanostatic charge was performed by a MACCOR series 4000 battery test system in a chamber set at 30 °C with maximum fluctuation of ± 0.1 °C using 2 hours of rest before test. Lithium stripping/deposition tests were carried out either on Li|50 μL catholyte |Li or Li|50 μL DOL:DME 1:1, 1m $LiNO_3$, 1m LiTFSI|Li symmetrical cells through galvanostatic cycling measurements, applying a constant current of 2.0 mA cm^{-2} and setting a step time of 2 h for both charge (stripping) and discharge (deposition) processes. Additional high-current Li-stripping/deposition test was carried

out on Li|50 μL catholyte|Li by applying various currents, namely 10, 20, 40, 60, and 100 mA cm^{-2}, before lowering back to 10 mA cm^{-2}, and setting a step time of 1 h for both charge and discharge (first and second currents were applied for 8 and 6 days, respectively, while subsequent ones were applied for 4 days). The cells were assembled by stacking two 14 mm-diameter Li discs separated by one 18 mm-diameter membrane (Celgard 2500) soaking either the catholyte or the reference solution. The stripping/deposition measurements were carried out using a MACCOR series 4000 battery test system, in a chamber set at 30 °C, with maximum fluctuation of ± 0.1 °C. Prior to the test, the cells were rested for 2 h. All the Nyquist plots recorded by EIS were fitted through non-linear least-squares (NLLS) method with the aid of the Boukamp software (see refs 11 and 12 in Manuscript) and only fits with a χ^2 value of the order of 10^{-4} or lower were considered appropriate. The fitting allows to describe the Nyquist spectra in terms of equivalent circuits, identified by the $R_e(R_iQ_i)Q$ model, including resistive (*R*) and capacitive (*Q*) elements. Specifically, R_e represents the electrolyte resistance and is indicated by the high-frequency intercept of the plot, (R_iQ_i) elements are associated to the high-medium frequency semicircle, and Q is the contribute due to constant phase elements, often identified by Q_w, indicating the semi-infinite Warburg-type Li^+ ions diffusion which is observed as a tilted line at low frequency (see refs 11 and 12 in Manuscript).

Sulfur-based electrodes

Three different sulfur-based materials, namely S:MnO_2 (80:20), S:Sn (80:20), and S:Sn:MnO_2 (80:10:10) were prepared through a solvent-free procedure reported in our previous works (see refs 7, 23, 24 in Manuscript). In brief, Sulfur, Sn, and/or MnO_2 were mixed, heated at 125 °C under magnetic stirring until complete melting of S, quenched at room temperature and grounded to obtain fine powders (round brackets in the above acronyms include the weight ratio of the components). Three cathode tapes were obtained through casting process with a doctor blade tool set at ~500 μm of a slurry formed by 80 wt.% of each active material powder, namely *(i)* S:MnO_2 (80:20), *(ii)* S:Sn (80:20), or *(iii)* S:Sn:MnO_2 (90:5:5), 10 wt.% PVDF polymer binder, and 10 wt.% few layer graphene

(FLG, produced by BeDimensional S.p.A., see ref 32 in Manuscript) as electron conductor, dispersed in N-methyl-2-pyrrolidone (NMP, Sigma-Aldrich). The slurries were cast on GDL foils, which were heated at 70 °C on a hot plate to remove the NMP solvent. Afterwards the tapes were cut with the aid of a 14 mm-diameter punch (1.54 cm^2 geometric area), and the electrodes were dried overnight at 30 °C under vacuum inside a Büchi oven, before being stored inside an Ar-filled glovebox. The S loading in the electrodes ranged from 0.7 to 2.7 mg cm^{-2}

Application in lithium cell

The catholyte solution was initially tested in CR2032 coin-type (MTI corp.) lithium cells exploiting the cathodes reported above. The typical cell was assembled by stacking a 14 mm lithium disc (0.25 mm thick, MTI corp.) separated by 18 mm-diameter membrane (Celgard 2500) from a 14 mm-diameter sulfur-based electrode soaked with 66 µL of catholyte solution (containing 5.8 mg of S). The overall active material content in the cells was calculated by adding the sulfur content of the catholyte to the one in the electrode, and was made explicit in each figure caption in which the two S-sources were employed. The cells were galvanostatically cycled in the 2.1 – 2.8 V voltage range at C/2. Additionally, the S:Sn:MnO_2 electrode was cycled within 2.1 – 2.8 V at C/10, C/5, C/3, C/2, and 1C, within the 2.0 – 2.9 V at 2 C, within 1.5 − 3.0 V at 5 C, 6 C, 7 C, 8 C, and 9 C, and within 0.5 − 3.5 V at 10 C, 20 C, 30 C, 40 C, and 50 C. The same cell was also subjected to CV measurement by scanning the potential at increasing rates, namely, 5, 6, 7, 8, 9, and 10 mV s^{-1} (3 cycles for each scan rate) in the 1.4 – 3.2 V *vs.* Li^+/Li potential range to determine the Li^+ diffusion coefficient D_{Li+} by using the Randles–Sevcik equation (3 in Manuscript). Prior to this test, the cell was subject to LSV from the cell OCV to 3.2 V *vs.* Li^+/Li, using a scan rate of 5 mV s^{-1}. The galvanostatic cycling measurements were performed via a MACCOR series 4000 battery test system, in a chamber set at 30 °C with maximum fluctuation of ±0.1 °C, while LSV and CV were carried out by using a VersaSTAT MC Princeton Applied Research (PAR-AMETEK) instrument at room temperature (25 °C) Before any test, all cells were rested for 2 h inside the chamber, and the first step of the test always

consisted in a stabilization charge run (formation cycle) at 0.1 C to 2.8 V. The estimation of the specific discharge power and energy refers to the content of sulfur in each cell. The 1 C rate (419 mA g_S^{-1}) was calculated considering the electrochemical conversion of S_8 to Li_2S_4 (i.e., S_8 + 4 Li → 2 Li_2S_4).

Figure S2a shows the Nyquist plot related to EIS spectra collected at various temperatures, namely from 0.0 °C to 64.5 °C, to determine the ionic conductivity of the catholyte solution reported in Figure 1a in Manuscript. A stainless-steel|catholyte solution|stainless-steel coin cell configuration was used. The bulk resistance was calculated from the corresponding EIS spectra through NLLS fitting (read beneath for details, and see refs 11 and 12 in Manuscript), and the ionic conductivity was calculated based on the equation:

$$\sigma = \frac{l}{R_b \times A}$$

where σ is the ionic conductivity (S cm^{-1}), R_b is the bulk resistance of the electrolyte (derived from the fitting), l is the O-ring thickness (127 μm, i.e., 0.0127 cm) and A is its internal geometric area (0.785 cm^2). The EIS spectra recorded to investigate the aging of the lithium/catholyte interphase are reported in Figure S2b, while Figure S2c depicts the corresponding interphase resistance trend during time evolution. The results of the NLLS fitting of the Nyquist plots in Figure S2b are reported in Table S1 (see refs 11 and 12 in Manuscript).

Figure S2d reports the galvanostatic charge profile of Li|catholyte |Carbon cell recorded at C/10 (1 C = 419 mA g_S^{-1}) before the CV test of Figure 1d (Manuscript), while Figure S2e shows the LSV carried out prior to CV of Figure 2e (Manuscript), both performed to activate the cell interphase.

Figure S2f depicts an insight of the stripping/deposition test of Figure 1e (Manuscript) evidencing a magnification of the trend between the 90th and 96th day.

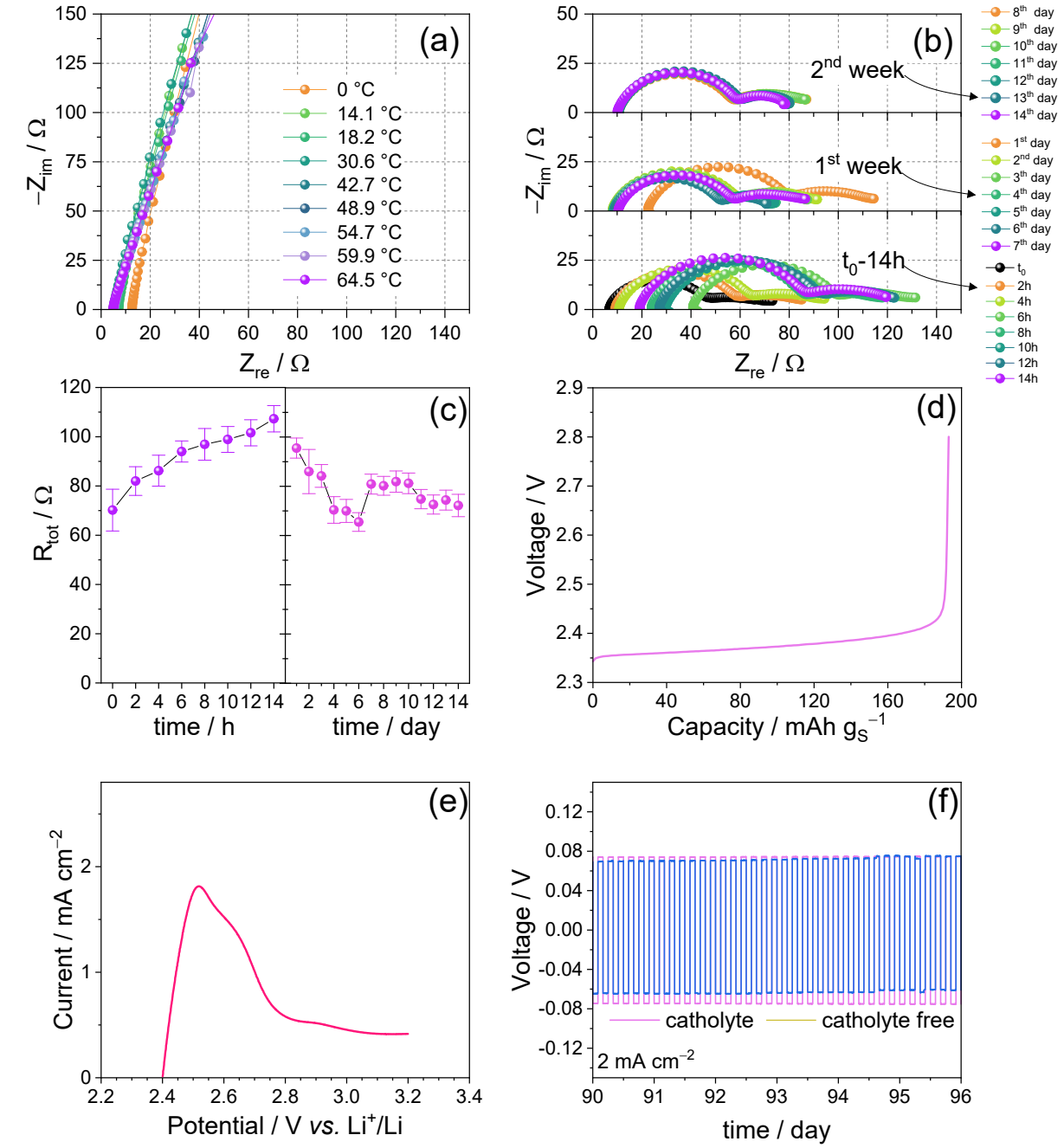

Figure S2. Electrochemical characterization of the catholyte, in detail: **(a)** Nyquist plots related with EIS measurements performed at various temperatures on a stainless-steel|catholyte solution|stainless-steel symmetrical cell to evaluate the ionic conductivity (see Figure 1a in Manuscript); frequency range: 500 kHz – 100 Hz, alternate voltage signal: 10 mV; **(b)** Nyquist plots recorded through EIS regularly measured upon aging of a Li|catholyte|Li symmetrical cell at room temperature, monitored during the initial 14 h (bottom panel), first week (middle panel), and second week (top panel) after assembling; frequency range: 500 kHz – 100 mHz, alternate voltage signal: 10 mV; **(c)** Resistance trend *vs.* time achieved by regularly carrying out EIS during aging of a Li|catholyte|Li symmetrical cell, applying the experimental constrains described above; initial 14 h (left panel), first and second week (right panel), see corresponding Table S1 for NLLS analyses (see refs 11 and 12 in Manuscript); **(d)** galvanostatic charge profile of Li|catholyte|Carbon cell recorded at C/10 (1 C = 419 mA g_S^{-1}) before the CV test of Figure 1d in Manuscript; **(e)** LSV carried out prior to CV in Figure 2e in Manuscript; **(f)** insight of the stripping/deposition within the 90th and 96th day (test reported in Figure 1e in Manuscript). Test performed at 25 °C.

Table S1. NLLS analyses performed on the Nyquist plots reported in Figure S2b recorded by EIS on a Li|catholyte|Li symmetrical cell upon aging at room temperature. The NLLS fitting was carried out with the aid of the Boukamp software (see refs 11 and 12 in Manuscript); the corresponding resistance trend with respect of time is displayed in Figure S2c.

Cell Condition	Circuit	R_1 [Ω]	R_2 [Ω]	$R_{tot} = \sum R_i$ [Ω]	χ^2
After assembly	$R_e(R_1Q_1)(R_2Q_2)Q$	34.1 ± 2.8	36.1 ± 1.4	70.2 ± 4.2	3×10^{-4}
After 2 hours	$R_e(R_1Q_1)(R_2Q_2)Q$	36.2 ± 1.8	45.8 ± 0.9	82.0 ± 2.7	1×10^{-4}
After 4 hours	$R_e(R_1Q_1)(R_2Q_2)Q$	34.1 ± 1.7	52.1 ± 0.8	86.2 ± 2.5	9×10^{-5}
After 6 hours	$R_e(R_1Q_1)(R_2Q_2)Q$	37.4 ± 1.3	56.6 ± 0.6	94.0 ± 1.9	2×10^{-5}
After 8 hours	$R_e(R_1Q_1)(R_2Q_2)Q$	36.1 ± 1.8	60.8 ± 0.8	96.9 ± 2.6	7×10^{-5}
After 10 hours	$R_e(R_1Q_1)(R_2Q_2)Q$	37.2 ± 1.5	61.7 ± 0.7	98.9 ± 2.2	4×10^{-5}
After 12 hours	$R_e(R_1Q_1)(R_2Q_2)Q$	38.7 ± 1.6	62.9 ± 0.7	101.6 ± 2.3	5×10^{-5}
After 14 hours	$R_e(R_1Q_1)(R_2Q_2)Q$	41.9 ± 1.6	64.7 ± 1.0	106.6 ± 2.6	7×10^{-5}
After 1 day	$R_e(R_1Q_1)(R_2Q_2)Q$	39.9 ± 1.3	55.6 ± 0.6	95.5 ± 1.9	4×10^{-5}
After 2 days	$R_e(R_1Q_1)(R_2Q_2)Q$	37.5 ± 2.9	48.7 ± 1.3	86.2 ± 4.2	4×10^{-4}
After 3 days	$R_e(R_1Q_1)(R_2Q_2)Q$	36.9 ± 1.2	47.3 ± 0.6	84.2 ± 1.8	2×10^{-4}
After 4 days	$R_e(R_1Q_1)(R_2Q_2)Q$	27.3 ± 1.4	43.1 ± 0.7	70.4 ± 2.1	3×10^{-4}
After 5 days	$R_e(R_1Q_1)(R_2Q_2)Q$	26.3 ± 1.3	43.7 ± 0.7	70.0 ± 2.0	2×10^{-4}
After 6 days	$R_e(R_1Q_1)(R_2Q_2)Q$	23.7 ± 1.2	41.8 ± 0.6	65.5 ± 1.8	1×10^{-4}
After 7 days	$R_e(R_1Q_1)(R_2Q_2)Q$	36.1 ± 1.3	44.8 ± 0.6	80.9 ± 1.9	9×10^{-5}
After 8 days	$R_e(R_1Q_1)(R_2Q_2)Q$	35.3 ± 1.2	44.9 ± 0.5	80.2 ± 1.7	8×10^{-5}
After 9 days	$R_e(R_1Q_1)(R_2Q_2)Q$	35.9 ± 1.4	46.0 ± 0.6	81.9 ± 2.0	1×10^{-4}
After 10 days	$R_e(R_1Q_1)(R_2Q_2)Q$	35.1 ± 1.4	46.1 ± 0.6	81.2 ± 2.0	9×10^{-5}
After 11 days	$R_e(R_1Q_1)(R_2Q_2)Q$	26.3 ± 1.1	48.5 ± 0.5	74.8 ± 1.6	9×10^{-5}
After 12 days	$R_e(R_1Q_1)(R_2Q_2)Q$	25.1 ± 1.0	47.5 ± 0.5	72.6 ± 1.5	9×10^{-5}
After 13 days	$R_e(R_1Q_1)(R_2Q_2)Q$	25.2 ± 1.1	49.2 ± 0.5	74.4 ± 1.6	1×10^{-4}
After 14 days	$R_e(R_1Q_1)(R_2Q_2)Q$	24.6 ± 1.3	47.6 ± 0.7	72.2 ± 2.0	2×10^{-4}

Figure S3 displays the galvanostatic cycling results of Li-S cells exploiting the catholyte in combination with each of the three sulfur-based cathodes, namely S:MnO_2, S:Sn, and S:Sn:MnO_2 (see experimental section above, and refs 7, 23, 24 in Manuscript). The aim of this test, carried out at C/2 (1 C = 419 mA g_S^{-1}) within the 2.1 – 2.8 V voltage range, is to determine the most suitable trade-off among the materials basing on the delivered specific capacity, sulfur content in the cathodic active material, and voltage profiles stability (see Manuscript for data interpretation).

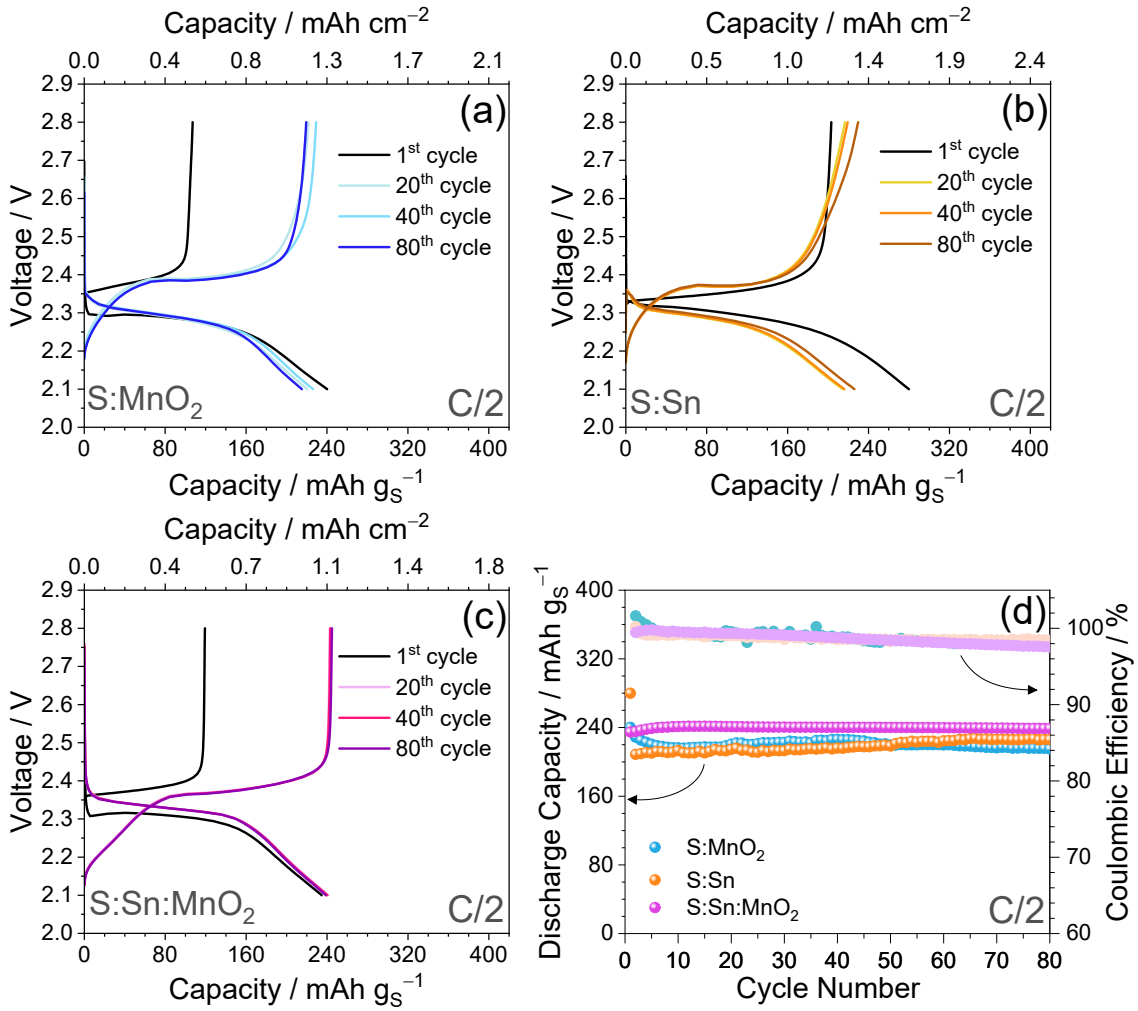

Figure S3. Galvanostatic cycling performance of the catholyte in lithium half-cell exploiting various sulfur-based cathode (see refs 7, 23, 24 in Manuscript). In detail: **(a)** selected voltage profiles of Li|catholyte|S:MnO_2 (80:20 *w:w)*, cell (top *x*-axis display the areal capacity); **(b)** selected voltage profiles of Li|catholyte|S:Sn (80:20 *w:w*) cell (top *x*-axis display the areal capacity); **(c)** selected voltage profiles of Li|catholyte|S:Sn:MnO_2 (90:5:5 *w:w*) (top *x*-axis display the areal capacity); **(d)** capacity trends comparison upon 80 charge/discharge runs (right *y*-axis shows Coulombic Efficiency). All cells were cycled at the constant rate of C/2 (1C = 419 mA g_S^{-1}) between 2.1 – 2.8 V. Each cathode was soaked with 66 µL of catholyte. Electrodes geometric area: 1.54 cm^2. Overall sulfur loading between 4.5 and 6.0 mg cm^{-2}.

The composition Li_2S_4 upon galvanostatic discharge of the liquid polysulfide is reached only in the theoretical case at very low current, such as the one reported in panel (a) of Figure S4. Instead, polysulfides having lower Li content are achieved by increasing the c-rate, such as Li_xS_8 with $3.2 \leq x \leq 2.4$ from C/10 to 1 C (panel b), $1.2 \leq x \leq 0.6$ from 5 C to 9 C (panel c), and $0.6 \leq x \leq 0.1$ from 10 C to 50 C (panel d).

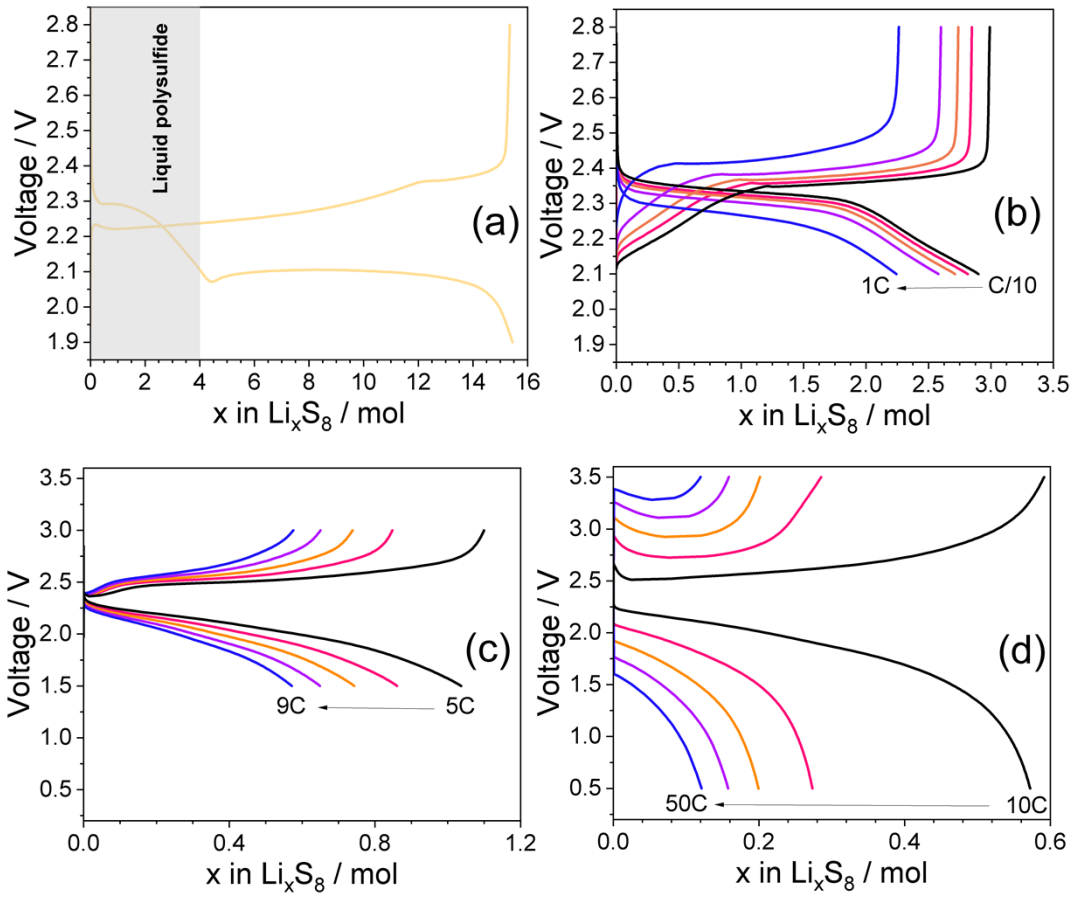

Figure **S4**. **(a)** Theoretical galvanostatic voltage profile of the Li-S cell at very low current in terms of exchanged Li moles (x) in the Li_xS_8 polysulfide formula highlighting the liquid region until Li_2S_4, and galvanostatic cycling tests of the cells reported in this work at: **(b)** C/10, C/5, C/3, C/2, and 1 C (1 C = 419 mA g_S^{-1}, S loading 6.5 mg cm^{-2}) in the 2.1 – 2.8 V voltage range; **(c)** 5 C, 6 C, 7 C, 8 C, and 9 C (S loading 5.2 mg cm^{-2}) in the 1.5 – 3.0 V voltage range; (d) 10 C, 20 C, 30 C, 40 C, and 50 C (S loading 5.2 mg cm^{-2}) in the 0.5 – 3.5 V voltage range.

Figure S5 summarizes the specific current (either in terms of mA g_S^{-1} or mA cm^{-2}) and discharge capacity delivered by Li|catholyte|S:Sn:MnO_2 cells upon rate capability tests, and depicts the linear fit of the peak current intensities (I_p) plotted *vs.* the square root of the scan rate ($v^{1/2}$) related to the CV measurements performed at increasing v (see Figure 2e in Manuscript) to estimate the Li^+ diffusion coefficient (D_{Li+}) by using the Randles-Sevcik equation (equation 3, references 25 and 26 in Manuscript). The obtained D_{Li+} values are reported in Table S2. See Manuscript for discussion.

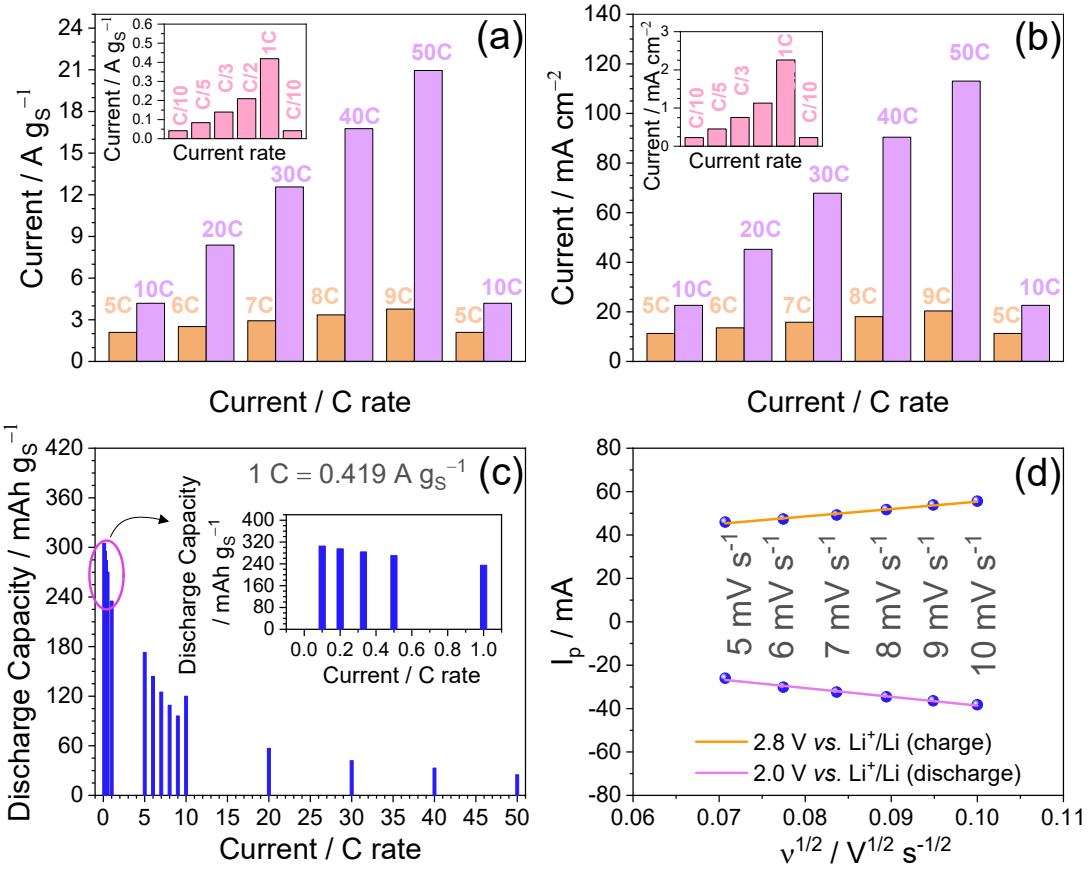

Figure S5. Rate capability tests performed in Li|catholyte|S:Sn:MnO_2 cell. In detail: **(a)** specific current (A g_S^{-1}) *vs.* current rate (C-rate); **(b)** areal current (mA cm^{-2}) *vs.* C-rate; **(c)** specific discharge capacity (taken at the 3rd discharge run for each current rate) *vs.* C-rate; **(d)** linear fits of the peak currents (I_p) vs. the root square of the scan rate ($v^{1/2}$) employed for the CV measurements reported in Figure 2e (Manuscript). The linear fit slopes are employed to calculate the Li^+ diffusion coefficient (D_{Li+}) values through the Randles-Sevcik equation (equation 3, references 25 and 26 in Manuscript). See Table S2 for the actual D_{Li+} values.

Table S2. Li^+ diffusion coefficient (D) values measured through the Randles-Sevcik equation (equation 3, and references 25 and 26 in Manuscript) during CV measurements of Li|catholyte |S:Sn:MnO_2 cell. See Figure 2e (Manuscript) and Figure S4c for details.

Potential / V *vs.* Li^+/Li	D / cm^2 s^{-1}
2.0	5.8×10^{-8}
2.8	4.2×10^{-8}

Figure S6 shows selected voltage profiles and capacity trends of the galvanostatic tests performed on Li|catholyte|S:Sn:MnO_2 cell at a current of 2 C (Figure S6a, b) and 6 C (Figure S6c, d), and Li stripping/deposition test performed in Li|catholyte|Li cell at increasing currents (Figure S6e). The aim of the test is to determine the specific power and cycling stability of the battery, and to check the effects of high currents on Li stripping/deposition polarization and stability. See Manuscript for detailed discussion.

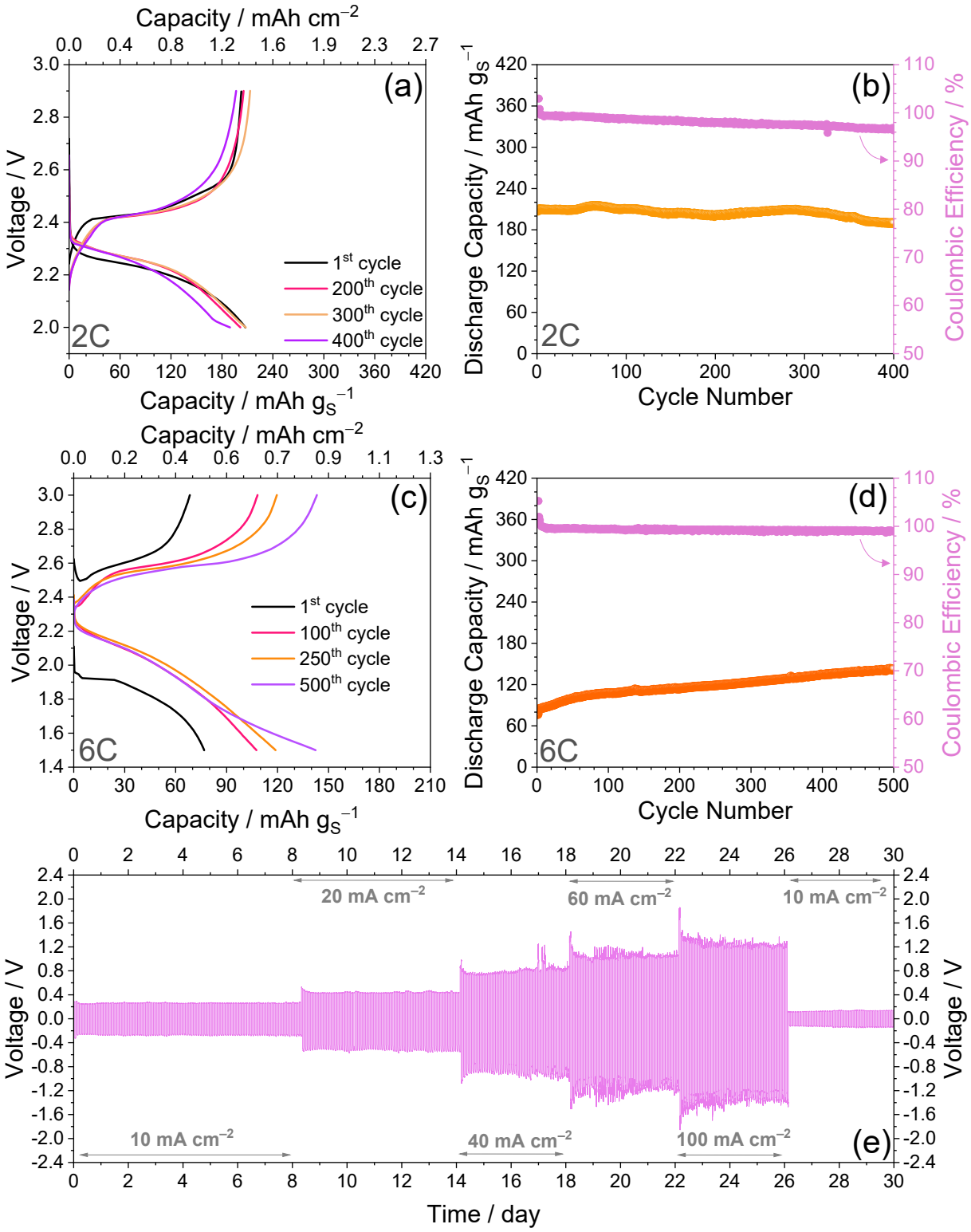

Figure S6. Galvanostatic cycling of Li|catholyte|S:Sn:MnO_2 cell at various current rate and Li stripping/deposition test performed in Li|catholyte|Li at increasing currents. The test at 2 C (1 C = 0.419 mA g_S^{-1}) and 6 C are reported in terms of: **(a, c)** selected voltage profiles (top *x*-axes report areal capacity), and **(b, d)** capacity trends (right *y*-axes report Coulombic Efficiency); voltage range: 2.0 – 2.9 V (2 C), 1.5 – 3.0 V (6 C); sulfur loading 5.4 mg cm^{-2} and 6.2 mg cm^{-2}, respectively (electrode geometric area: 1.54 cm^2); **(e)** Li-stripping/deposition test at the constant currents of 10, 20, 40, 60, and 100 mA cm^{-2}, before lowering back to 10 mA cm^{-2} after 26 days, step time: 1 h. Tests performed at 30 °C.

Taking into account exclusively the voltammetry result of Figure 1c in the Manuscript (purple line) we may expect irreversible electrolyte reduction below 1.0 V, which can typically affect the electrochemical performance of the cell. However, the reaction takes place with an overvoltage exceeding 0.5 V at C-rate higher than 10 C as indicated by Figure S5e. Therefore, the DOL and DME decomposition may occur at high currents beside the 0.5 − 3.5 V voltage range, which is indeed the one selected for the tests from 10 C to 50 C in Figure 2c in the Manuscript without negative effects on the cell performance. On the other hand, possible slight electrolyte decomposition indicated by coulombic efficiency different than 100 % may contribute to the formation of a SEI layer that can potentially stabilize the cell behavior and avoid further side processes.

The Figure S7 reports a Ragone plot alternative to the one of Figure 3d (Manuscript), with energy and power densities reported on the y-axis (left and right) and the C-rate on the x-axis.

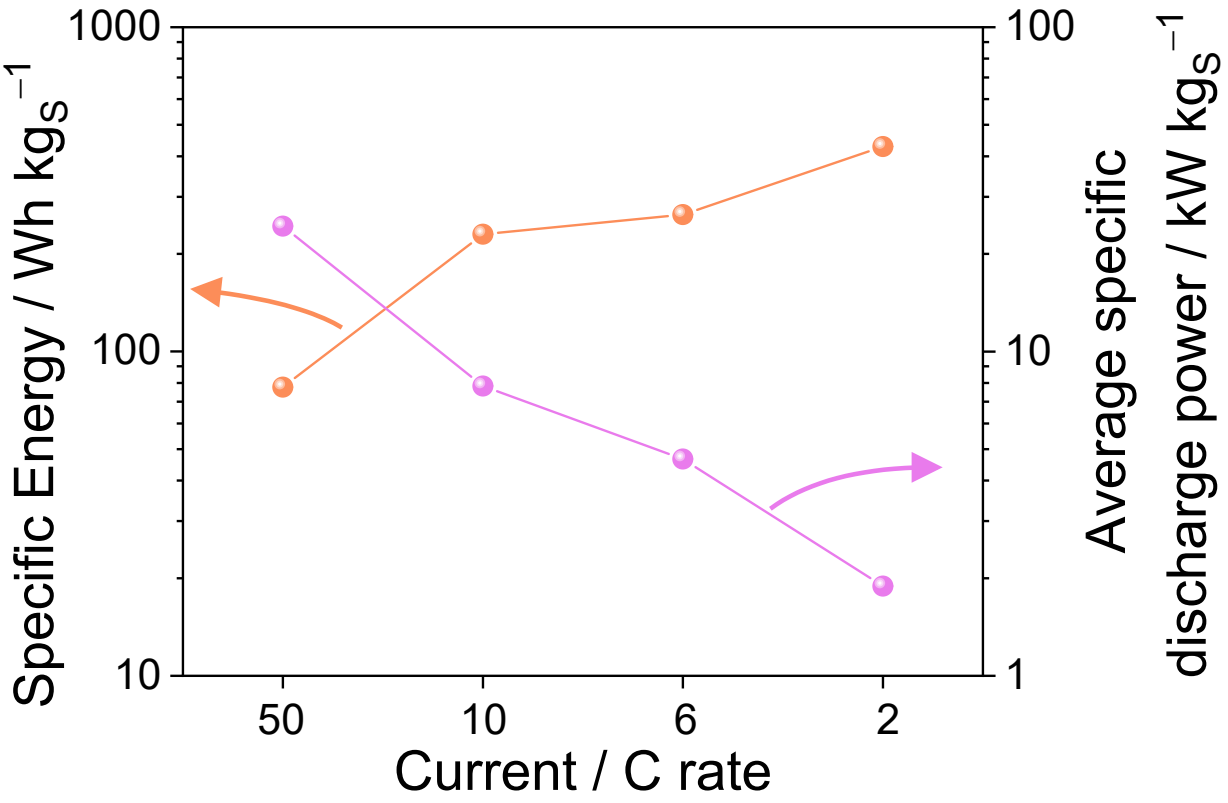

Figure S7. Specific energy (left *y*-axis) and average specific discharge power (right *y*-axis) vs. C-rate, data taken from the last discharge run of the long term galvanostatic cycling tests reported in Figure 3 (Manuscript) and Figure S6.